A NUMERICAL SIMULATION OF HYPERVELOCITY IMPACT OF SPACE DEBRIS AGAINST THE WHIPPLE BUMPER SYSTEM

Masahide Katayama*, Tatsuhiko Aizawa**, Seishiro Kibe*** and Susumu Toda***

*Structural Dept., CRC Research Inst., Inc., Chiba, Japan
**Dept. of Metallurgy, Univ. of Tokyo, Tokyo, Japan
***Structural Mechanics Div., NAL, Tokyo, Japan

ABSTRACT

On the basis of actual space station design, both analytical model and method was presented for numerical simulation of space debris hypervelocity impact against double–sheet structures: Whipple bumper system. Two dimensional explicit finite difference code was utilized together with an equation of state for three phases. The effectiveness and validity of an interactive Lagrangian rezoning method was demonstrated by good agreement with multiple material Eulerian method.

Key Words: Hypervelocity Impact, Whipple Bumper, Shock–Induced Vaperization, Debris Cloud, Hydrocode, Interactive Rezoning

1.INTRODUCTION

The spacecrafts are exposed to hazards of the impact by orbital space debris at upto about 15 km/s. The experimental methods have difficulties in investigating the integrity of the structures of spacecrafts mainly from two reasons: 1) current test capabilities are limited to impact velocities of about 10 km/s, and 2) the transient and interior changes in the materials are still unknown. Then the numerical analysis approach is of great importance to predict overall structural responses and to understand the mechanism of hypervelocity impacts.

When solid materials impacting structures at over 10 km/s, almost all materials used for both projectiles and targets might be vaporized to form debris clouds. From the viewpoint of the protection design, the sacrificial bumper was suggested for the purpose of decreasing the damage of rear main structure through the shock–induced vaporization process of itself, as depicted in Fig. 1. Although this method was first suggested by F. L. Whipple (Ref. 1) in order to protect spacecrafts against the meteoroid impact, it is also useful for the shielding of the space debris. On the other hand, for hypervelocity impact problems is indispensable the equation of state covering solid, liquid and gas phases at the same time. Several studies were carried out for this purpose (Refs. 2, 3, 4). In this study, we offer both analytical model and method for space debris impact against double–sheet structures based on an actural space station design, utilizing two–dimensional explicit finite difference hydrocode and an equation of state applicable for three phases.

2.ANALITICAL MODEL

An axisymmetric analytical model was employed on the basis of actual design of a Whipple shield system, as shown in Fig.2. together with several geometric parameters. A cylindrical space debris

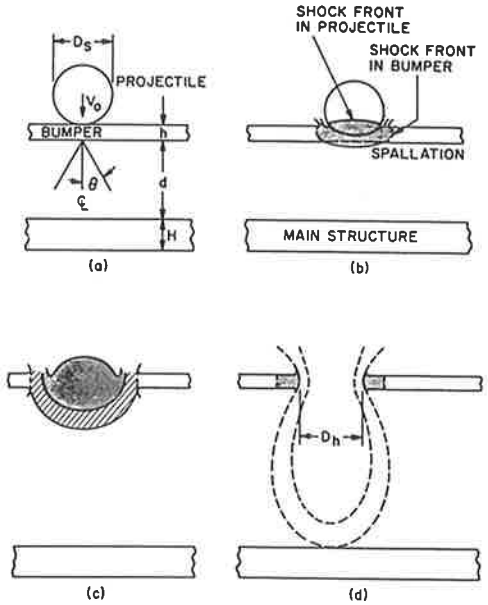

Figure 1. Schematics depicting (a) the impact onto a thin bumper plate, (b) its penetration, (c) the subsequent formation of a spallation cone, and (d) the loading transmitted by the cone to the main structure downstream.
(From " High–Velocity Impact Phenomena" Ed. by R. Kinslow)

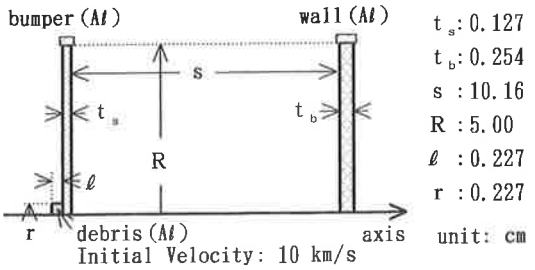

Figure 2. Analytical Model

with a height of 0.227 cm, a radius of 0.227 cm and a mass of 0.1 g is assumed to have an initial impact velocity of 10 km/s. The outer egdes of both bumper and main wall were restrained.

Tillotson's equation of state and elastic–perfectly–plastic constitutive model for pure aluminum were applied to the first bumper, the main wall and the space debris. This equation of state consists of two different analytical formulas. One describes materials in compression and expansion regimes at the energies less than the sublimation energy E_s and at the densities between a critical density ρ_s and a reference density ρ_0. The other describes materials in the rest of expansion regime. The constants of the equation for the former part, for relatively 'low' pressure (< 1 TPa) region, come from the shock Hugoniot data in Los Alamos National Laboratory. The latter constants, for 'high' pressure region, are derived by means of the Thomas–Fermi statistical theory of the atom. The same material properties were used for the three components; the parameters for the equation of state were quoted from reference 2, and for yield stress, shear modulus, ultimate strain and spalling pressure were assumed to be 50 MPa, 27.6 GPa, 40% and −0.2 GPa respectively.

3. METHOD

In the hydrodynamic codes (hydrocodes), two different solution schemes are mainly employed: Lagrangian and/or Eulerian schemes. In the Lagrangian scheme the numerical mesh moves and distorts together with the material motions. The material flows through a fixed numerical mesh in the Eulerian. For the simulation of hypervelocity impact phenomena inducing vaporization, generally speaking, the Eulerian frame of reference is rather suitable than the Lagrangian. This is partially because the original mesh is often severely distorted by complicated deformation. One of authors proposed a simulation method of iron–aluminum hypervelocity impact by multiple material Eulerian solution scheme, and showed that it is very effective to comprehend the mechanism of the hypervelocity debris impact against the double–sheet structure (Ref. 5). However, in the analytical model the distance between the two sheets was much closer than that of the actual design. As shown in Fig.2, the actual distance is 80/40 times longer than the thickness of Whipple bumper/main structure. If we would make Eulerian meshes for the whole system shown in Fig.2 with enough accuracy, over 200,000 meshes and over 10,000 times time–integrations might be required. It might take over 200 hours by the current supercomputer to carry out such a calculation. To cope with this problem, we decided to apply the Lagrangian frame of reference to all components by proceeding several interactive rezonings for seriously distorted portions in the present study. Two–dimensional explicit finite difference hydrocode: AUTODYN–2D (Ref. 6) was used for the calculations. Both Lagrangian processor with an interactive rezonig capability and multiple material Eulerian processor are available in this code. Especially this interactive rezoning capability enables us to carry out regridding and remapping much more quickly and easily than the conventional non–interactive rezoning procedures.

4. RESULTS AND DISCUSSIONS

Preceding to our main analysis, we compared the results during the first target perforation between by Lagrangian and Eulerian calculations. Fig.3 indicates the comparison of velocity vector distributions at 0.25 and 0.50 μs between Lagrangian and Eulerian approaches. The results at 0.25 μs show a good agreement, while the outlines of projectile and target materials at 0.50 μs show considerable differences seemingly. The material fraction contour at 0.50 μs in Eulerian calculation depicts that the difference was caused by material contour scheme for Eulerian processor. Fig.4 indicates the comparison of the energy balance histories between Lagrange and Euler. These figures also show a good agreement except that the internal energy in Lagrangian calculation is estimated lower than in Eulerian. This difference might be caused mainly by rezoning procedures which discard the seriouly distorted but unimportant zones. Fig.5 indicates the comparison of pressure histories at selected target points between Lagrange and Euler. The corresponding each history at target number 1, 3 and 4 has a good agreement, while that at target number 2 shows a difference in the skirt region. Since the Eulerian calculation was performed with about twice finer numerical meshes than Lagrangian, both target point locations do not correspond to each other exactly. As the pressure histories of Eulerian processor are produced by using tracer points (marker particles) technique, the curves are not smooth but rugged. The oscillations in the Lagrangian calculation might be caused by Lagrangian impact/slide scheme.

We continued with Lagrangian calculations after the first bumper perforation. Fig.6 depicts the dynamic processes untill the main structure impact and deformation. Fig.6a is drawn with the same scaling and the same velocity vector scaling. Fig.6b and c are zoomed velocity vector

distribution and density contour in the vicinity of first bumper impacting region at 0.60 μs. Fig.6b and c are drawn with ten times larger scaling than Fig.6a, as against with the same velocity vector scaling for Fig.6a and b. Fig.6d indicates the density contour at 9.46 μs: the instance of main structure impact. This figure tells us that both the debris and the wreckage of bumper material have already been expanded sufficiently to have the densities in gas phase. We can understand from this reason that the main structure is subjected to much smaller damages in Fig.6a than the first bumper impact. Fig.7 shows the final material status of the main structure. This figure indicates that both front and rear side of the main structure are failed in the vicinity of axis, and that this design is placed in a critical point from the viewpoint of main structure integrity.

5. CONCLUSIONS

Through the present simulation, our developed procedure was found to be an effective and efficient method to predict and understand overall structural responses of space debris hypervelocity impact against double–sheel structures. In our model, the total numerical meshes with Lagrangian processor are at most 1,000 and the time integration steps are only less than 2,500. We can perform such simulations sufficiently with engineering work stations. In the present approach, however, manpower performance was not so good as the multiple material Eulerian method, since a couple of hours were consumed by interacting rezoning procedures. Authors are ready to propose an automatic rezoning capability for morequick mesh refinement. The related paper will be reported in near future.

6.REFERENCES

1. Whipple, F.L., Physics and Medicine of the Upper Atmosphere (White, C.S. and Benson, O.O., Jr., eds.), pp. 137, Univ. of New Mexico Press, Albuquerque, 1952.

2. Tillotson, J.H., Metallic equations of state for hypervelocity impact, General Atomic Division of General Dynamics Report, GA–3216, 1962.

3. Thompson, S.L. and Lauson, H.S., Improvements in the CHARTD radiation hydrodynamic code III: reviced analytic equations of state, Sandia National Laboratories Report, SC–RR–71–0714, 1972.

4. Holian, K.S., T–4 Handbook of Material Properties Data Bases, Vol. Ic: Equation of State, Los Alamos National Laboratory Report, LA–10160–MS, 1984.

5. Katayama, M., A Numerical Simulation of Hypervelocity Impact Problem by A Hydrocode, Proc. of Space Debris Workshop'91, pp. 33, Japan Society for Aeronautical and Space Sciences & Inst. of Space and Astronautical Science, 1991.

6. Birnbaum, N.K. and Cowler, M.S., Comparison of Euler, Lagrange, ALE and Coupled Euler–Lagrange Calculations in Terminal Ballistics, Proc. 11th Int. Symp. on Ballistics, Brussels, 1989.

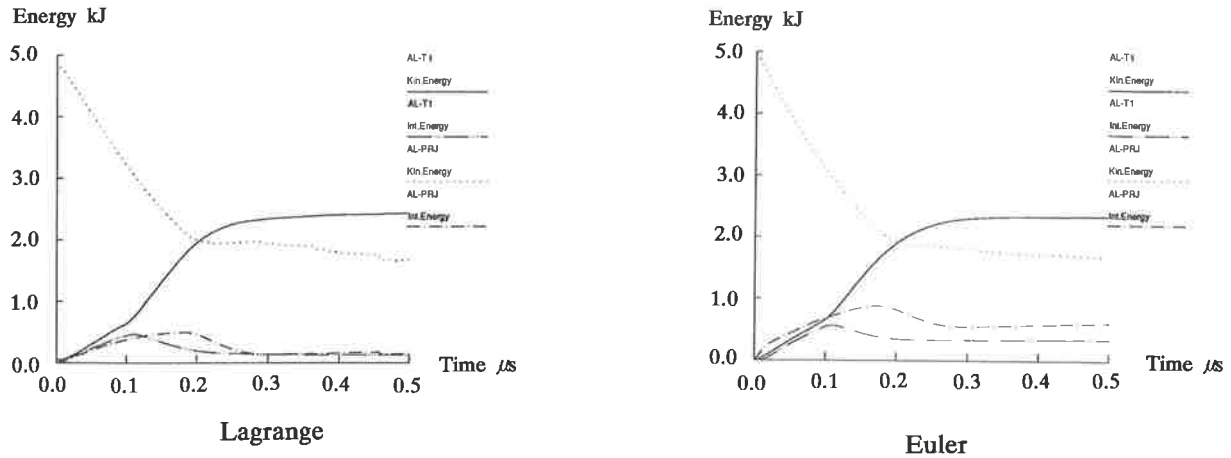

Figure 4 Energy balance history

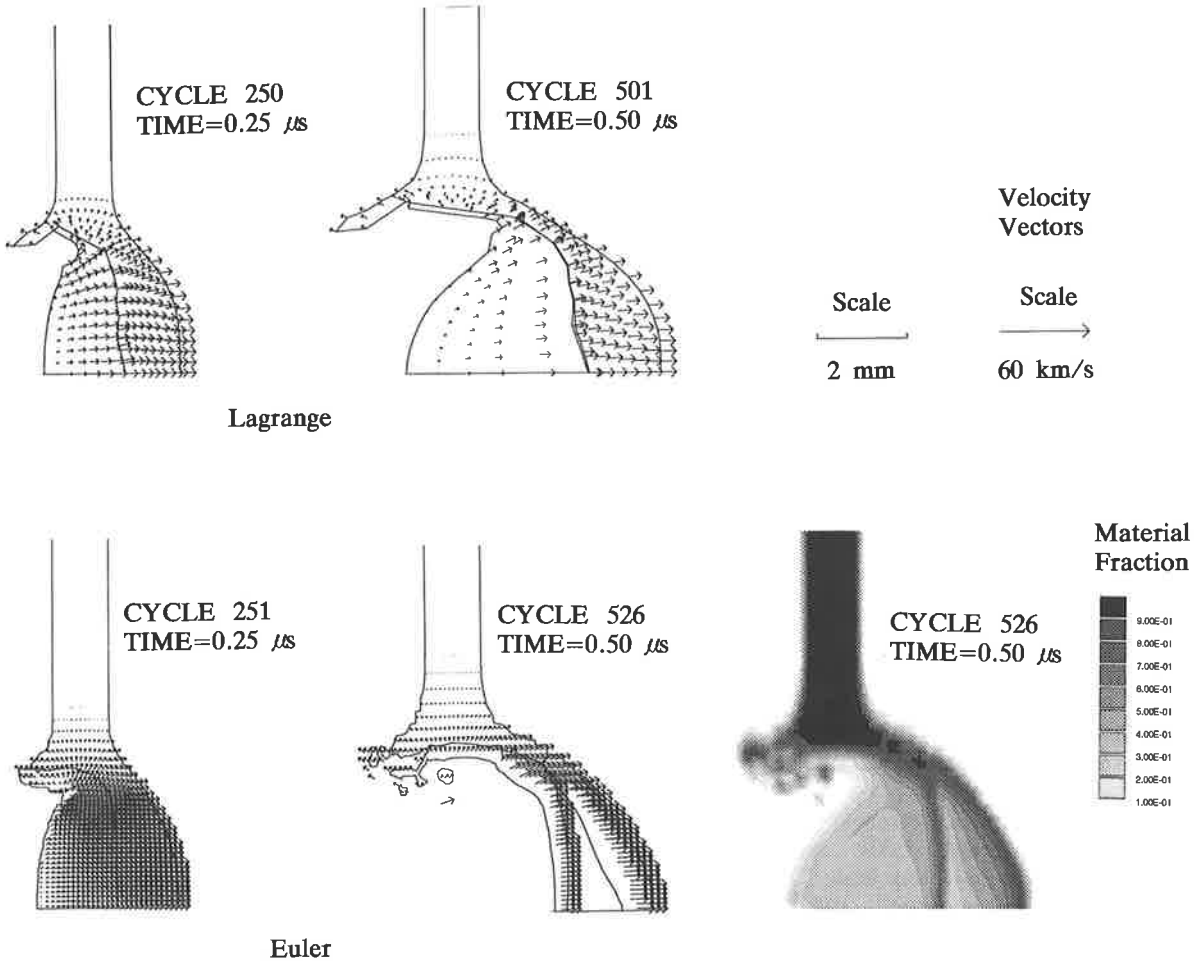

Figure 3 Comparison between Lagrangian and Eulerian results

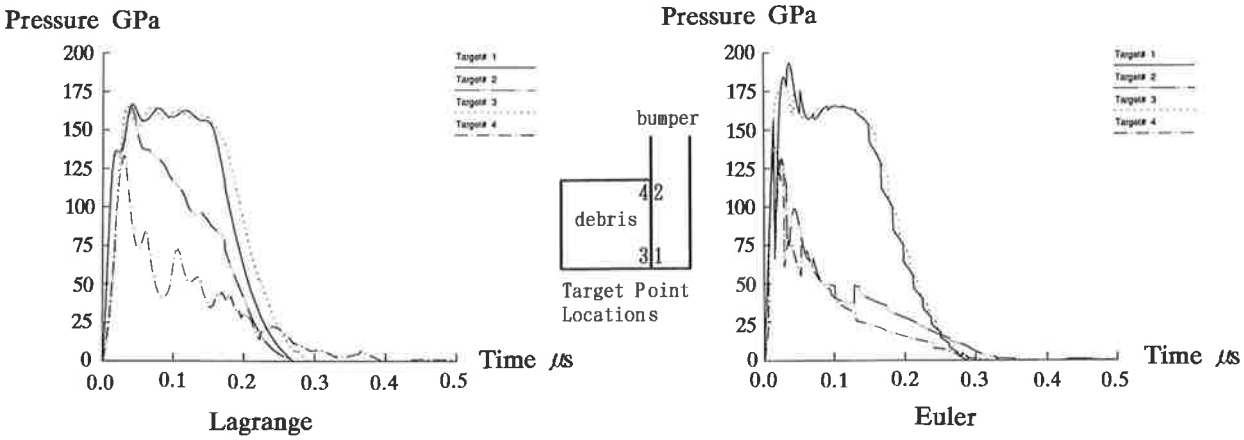

Figure 5 Pressure history

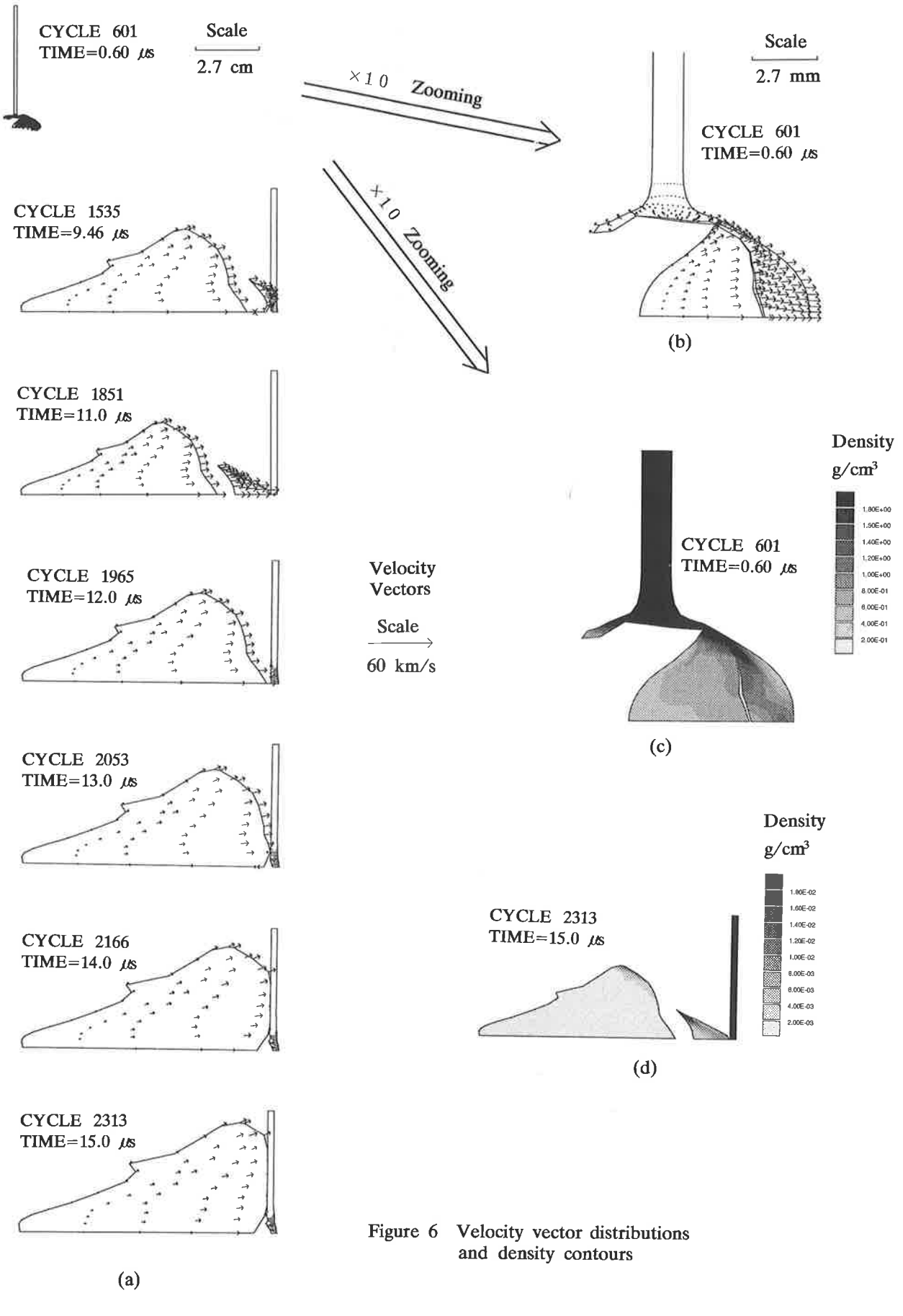

Figure 6 Velocity vector distributions and density contours

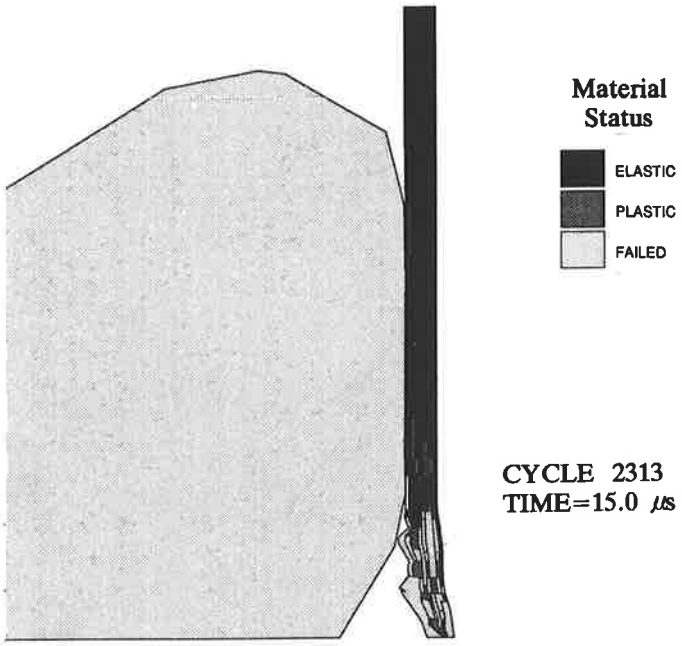

Figure 7 Material status of the main structure